Korean J. Chem. Eng., 33(3), 795-805 (2016)
DOI: 10.1007/s11814-015-0201-0

pISSN: 0256-1115
eISSN: 1975-7220

Effects of uniform magnetic field on the interaction of side-by-side rising bubbles in a viscous liquid

Amin Hadidi and Davood Jalali-Vahid†

Faculty of Mechanical Engineering, Sahand University of Technology, Tabriz, Iran
(*Received 2 July 2015 • accepted 19 September 2015*)

Abstract−Effects of uniform magnetic fields on the interaction and coalescence of side-by-side rising bubbles of dielectric fluids were not studied; so in the present research, effects of different strengths of uniform magnetic field on the interaction of two bubbles rising side by side in a viscous and initially stagnant liquid are studied, numerically. For numerical modeling of the problem, a full computer code was developed to solve the governing equations which are continuity, Navier-Stokes, magnetic field and interface capturing equations which are level set and re-initialization equations. The finite volume method is used for the discretization of the hydrodynamic equations where the finite difference method is used to discretization of the magnetic field equations. The results are compared with available numerical and experimental results which show a good agreement. It is found that the uniform magnetic field can be used for contactless control of side-by-side coalescence of bubbles.

Keywords: Uniform Magnetic Field, Coalescence, Bubble Pairs, Two-phase Flow, Side-by-side Rising Bubbles

INTRODUCTION

The behavior of rising gas bubbles, especially their interactions and coalescence with each other in bubbly flows, is significant in the study of two-phase flows in chemical reactors, bioreactors, aeration, distillation columns etc. [1]. Interaction of bubble pairs may result in coalescence, which is one of the most important phenomena occurring in bubble columns. The interaction and coalescence between bubbles in the liquid could motivate heat transfer, mass transfer and chemical reaction in gas-liquid systems [2]. As a consequence, many numerical and experimental studies of rising bubbles have been conducted. Among the earlier studies, Duineveld [3] studied the side-by-side air bubbles rising in in both pure water and aqueous surfactant solutions. He showed that there is a critical concentration of surfactants above which coalescence is inhibited. So, the added surfactant can be used as an agent to prevent bubbles from coalescence. Das and Pattanayak [4] investigated the transition of dispersed bubble to slug flow in a cryogenic two-phase flow. They pointed out that the coalescence of the bubbles affects the behavior of the flow by controlling the transition process. Therefore, coalescence of bubbles is an important parameter in the transition process. Ramos-Banderas et al. [5] studied two phase gas-liquid flows inside the submerged entry nozzle of a slab mold. They found that in the casting process, population and coalescence of the bubbles are important parameters which could affect the quality of the casting and materials produced by the casting process. Coalescence of the bubbles affects the behavior of the flow by controlling the transition in the regime of the flow. As the behavior of different regimes such as bubbly and slug regimes is fundamentally different, coalescence of bubbles can affect the regime of the flow and consequently its hydrodynamic specifications such as turbulence, wake, drag and also heat transfer specifications. So, by controlling the bubbles to coalesce with each other or preventing them from coalescence, the regime and specifications of the flow would be controllable. As an example of studies conducted on the control of the coalescence process, the study of Xie et al. [6] could be mentioned. They used acoustic and ultrasound waves to help water drops to coalesce and recover oil from water-oil (W/O) emulsions. They found that these waves can effectively enhance coalescence of the water droplets in an oil separation system. Alinezhad et al. [7] investigated separation of water in crude oil emulsion under non-uniform electric field. They showed that the applied electric field affects the coalescence process between the water droplets.

One of the novel and contactless methods for controlling the dynamics of bubbles is the application of external magnetic fields. Numerous studies have been carried out on the effects of whether uniform or non-uniform magnetic fields on the behavior of bubbles. However, investigations on the effects of uniform magnetic field on the dielectric flows are rare. Effects of uniform magnetic field on the dielectric two-phase flows were shown by Ki [8]. He showed the effects of an external uniform magnetic field on the dielectric single bubble and droplet for the first time. The effects of the uniform magnetic field on the coalescence of bubbles of fluids with low electrical conductivity such as air and water, have not been studied. As the shape and deformation of the interface in the coalescence process are very important phenomena, study of the effects of uniform magnetic fields which only acting on the interface and not affects the bulk of the liquid and gas phases can be very attractive, which has been investigated in the present research. The results of this research could be used in developing novel and superior methods for controlling the interactions and coalescence of bub-

†To whom correspondence should be addressed.
E-mail: amin.hadidi@yahoo.com, a_hadidi@sut.ac.ir, davoodjalali@sut.ac.ir

bles in industrial applications. Therefore, in this research, the effects of a uniform magnetic field on the interaction and coalescence of side-by-side rising bubbles in a liquid column where both of the fluids are dielectric are investigated for the first time.

DESCRIPTION OF THE PROBLEM

Our objective was to simulate the interaction of bubble pairs rising side by side in a viscous liquid column under the effects of a uniform magnetic field. Motion, interaction and coalescence of the bubbles were investigated under the effects of buoyancy force and an external uniform magnetic field. Both of the fluids (gas and liquid) are assumed to be incompressible and dielectric (have low electrical conductivity), and the magnetic permeability of the gas phase is assumed to be equal to the magnetic permeability of air, but the magnetic permeability of the liquid phase is twice the permeability of air [8]. The initial shape of bubbles is assumed to be spherical. Because rising bubbles in a stagnant liquid are investigated, stationary conditions were applied for the both phases as initial conditions. The geometry of the problem is shown schematically in Fig. 1.

To eliminate the effects of geometry's walls on the dynamics of bubbles, the distance between the center of the bubbles and the vertical walls must be more than three times the bubble radius [9]. In each case investigated in this research, first, a test of independency of the results from wall effects was conducted and appropriate dimensions of the column determined. However, for the validation of the results, dimensions of the column were set exactly to the dimensions considered by previous researchers for the sake of comparison. For this reason, minimum initial distance between bubbles' center and the vertical walls of the column is greater than three times of the bubble's initial radius in this simulation. Also, the column height should be large enough to make sure that the coalesced bubble can reach the terminal velocity and its steady shape. Therefore, the height of the column usually is determined by trial and error [10]. In this research, the height of the column is found to be ten times greater than the equivalent diameter of the coalesced bubble.

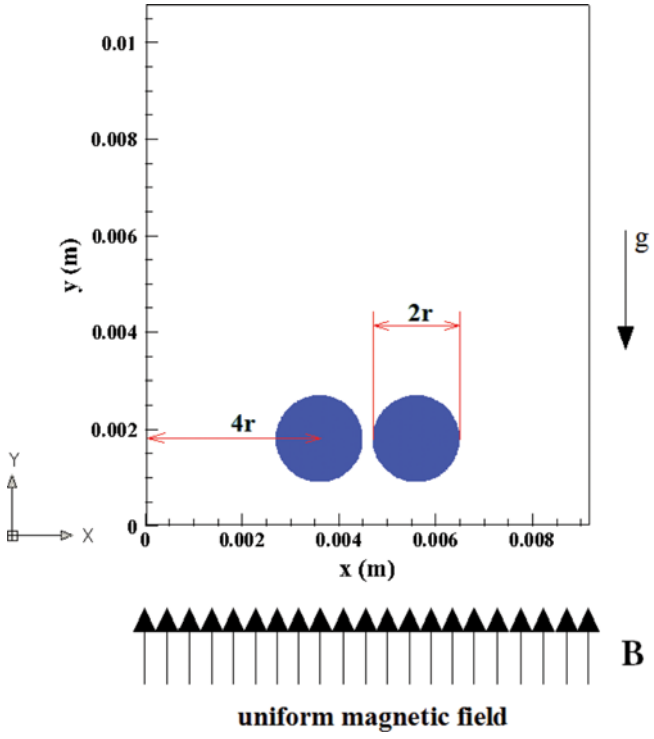

Fig. 1. Schematic geometry of the problem.

MATHEMATICAL MODELING

The governing equations of the two-phase bubbly flow under the effects of an external uniform magnetic field in this research consist of the conservation equations of continuity and momentum and the magnetic field equation, which is obtained by a simplification of Maxwell's equations. The level set equation is also added to the above-mentioned equations with re-initialization equations to capture the interface dynamics. Mentioned governing equations are presented in this section.

1. Flow Field Modeling

Governing equations of the flow field are continuity and the Navier-Stokes equations are presented, respectively, as below [8].

$$\vec{\nabla}\cdot\vec{V}=0 \tag{1}$$

$$\rho(\phi)\frac{D\vec{V}}{Dt}=-\vec{\nabla}p+\vec{\nabla}\cdot(2\mu(\phi)\overleftrightarrow{D})+\vec{F}+\vec{T}+\rho(\phi)\vec{g} \tag{2}$$

where $\vec{V}$, ϕ, p, ρ and μ are velocity vector, level set function, pressure, density and fluid viscosity respectively and also D/Dt is the substantial or total derivation. The surface tension force, gravity acceleration vector and the body force of the magnetic field are presented by $\vec{F}$, $\vec{T}$ and $\vec{g}$ respectively [11]. Term $\overleftrightarrow{D}$ is the rate of strain tensor and defined as below [11,12]:

$$\overleftrightarrow{D}=\frac{1}{2}[(\vec{\nabla}\vec{V})+(\vec{\nabla}\vec{V})^{T}] \tag{3}$$

2. Interface Modeling

In the level set method, the interface is represented by a function named as level set function. For every point within the flow field, the level set function can be calculated by the level set partial differential equation [11]:

$$\frac{\partial\phi}{\partial t}+\vec{V}\cdot\vec{\nabla}\phi=0 \tag{4}$$

The interface of two phases is defined by the zero contours of the level set function as follows [11]:

$$\Gamma=\{(x,y)|\phi(x,y,t)=0\} \tag{5}$$

Also, the nonzero values of the level set function indicate that the referred point belongs to the bulk of the gas or liquid phase. A summary of the level set function values at different points of the flow field in the multiphase flows is presented in Eq. (6) [13].

$$\phi(x,y,t)\begin{cases}>0 & (x,y)\in\text{liquid}\\ =0 & (x,y)\in\text{interface}\\ <0 & (x,y)\in\text{gas}\end{cases} \tag{6}$$

The physical properties of the fluids as a function of the level set parameter are presented as [14]:

$$\rho_\varepsilon(\phi)=\rho_g+(\rho_l-\rho_g)H_\varepsilon(\phi) \quad (7)$$

$$\mu_\varepsilon(\phi)=\mu_g+(\mu_l-\mu_g)H_\varepsilon(\phi) \quad (8)$$

$$\eta_\varepsilon(\phi)=\eta_g+(\eta_l-\eta_g)H_\varepsilon(\phi) \quad (9)$$

where $\eta(\phi)$ is the magnetic permeability of the fluid. Also $H_\varepsilon(\phi)$ is the Heaviside function defined in the level set formulation as [15]:

$$H_\varepsilon(\phi)=\begin{cases}0 & \phi<-\varepsilon\\ \frac{1}{2}\left[1+\frac{\phi}{\varepsilon}+\frac{1}{\pi}\sin\left(\frac{\pi\phi}{\varepsilon}\right)\right] & |\phi|\le\varepsilon\\ 1 & \phi>\varepsilon\end{cases} \quad (10)$$

In Eqs. (7) to (10) the parameter ε is the interface numerical thickness, which is proportional to the mesh size. Thickness of the interface is defined as [15,16]:

$$\varepsilon=\alpha\cdot\Delta x \quad (11)$$

where Δx is the size of the finest mesh. The suggested amount of α which was referenced in most of the articles is 1.5 (α=1.5) [14].

3. Magnetic Field Modeling

3-1. Magnetic Field Equations

Governing equations on the electromagnetic fields comprise four equations, Maxwell's equations. These equations include Gauss's law for electric fields, Gauss's law for magnetic fields, Faraday's law of induction and Ampere's law. In the absence of electric fields, Maxwell's equations are simplified to the two following equations [8].

The divergence equation (Gauss's second law) [8]:

$$\vec{\nabla}\cdot\vec{B}=0 \quad (12)$$

The curl equation (Ampere's law) [8]:

$$\vec{\nabla}\times\vec{H}=\vec{J}_c \quad (13)$$

In Eq. (12) and (13) $\vec{B}$, $\vec{H}$, η and $\vec{J}_c$ are the strengths of magnetic field in the fluid (magnetic flux density), magnetic permeability of the fluid, the strength of the applied external magnetic field, which is a function of the magnetic field generator and the electrical current, respectively. The relation between the strength of the externally applied magnetic field to the strength of the magnetic field after passing through the flow field which is dependent on the magnetic properties of the fluids is defined as [17]:

$$\vec{B}=\eta\vec{H} \quad (14)$$

A potential vector can be defined in the magnetic field vector $\vec{B}$ as [8]:

$$\vec{B}=\vec{\nabla}\times\vec{A} \quad (15)$$

The defined potential vector in Eq. (15) is not unique, but it was selected so as $\vec{\nabla}\cdot\vec{A}=0$. By making use of the defined potential vector in Eq. (15) and combining Eqs. (12) to (14), the magnetic field equation is written as [8]:

$$\frac{1}{\eta(\phi)}\vec{\nabla}\times\vec{\nabla}\times\vec{A}+\left(\vec{\nabla}\frac{1}{\eta(\phi)}\right)\times\vec{\nabla}\times\vec{A}=\vec{J}_c \quad (16)$$

For a two-dimensional coordinate system, the potential vector which was defined in Eq. (15) can be written as [8]:

$$\vec{A}=(0,\ 0,\ \xi) \quad (17)$$

By substituting the potential vector from Eq. (17) in Eq. (15), the magnetic field vector can be rewritten as [8,9]:

$$\vec{B}=\left(\frac{\partial\xi}{\partial y}\right)\vec{i}-\left(\frac{\partial\xi}{\partial x}\right)\vec{j} \quad (18)$$

where i and j are unit vectors in x and y directions, respectively.

As there is no electric current in the flow field, by substituting Eq. (17) in Eq. (16) and using Eq. (18), the governing equation for the magnetic field can be written as [8,9]:

$$\nabla^2\xi+\eta(\phi)\left(\frac{1}{\eta_g}-\frac{1}{\eta_l}\right)\delta(\phi)\vec{n}\cdot\nabla\xi=0 \quad (19)$$

where $\delta(\eta)$ is the delta function and $\vec{n}$ is the normal unit vector and defined as [15]:

$$\vec{n}=\frac{\vec{\nabla}\phi}{|\vec{\nabla}\phi|} \quad (20)$$

As the delta function has a sharp behavior, therefore, it should be smoothed as [15]:

$$\delta_\varepsilon(\phi)=\frac{dH_\varepsilon}{d\phi}=\begin{cases}0 & \phi<-\varepsilon\\ \frac{1}{2\varepsilon}+\frac{1}{2\varepsilon}\cos\left(\frac{\pi\phi}{\varepsilon}\right) & |\phi|\le\varepsilon\\ 0 & \phi>\varepsilon\end{cases} \quad (21)$$

3-2. Magnetic Field Force Term

Applied magnetic field to the flow domain will exert an induced force at the interface of two phases, which was presented by $\vec{T}$ in the momentum equation (Eq. (2)). The induced force could be modeled by adding a source term to the momentum equation, and it can be expressed as [8]:

$$\vec{T}=\left(\frac{1}{\eta_g}-\frac{1}{\eta_l}\right)B_n^2\delta(\phi)\vec{n}-\frac{1}{2}\left((\eta_g-\eta_l)H^2+\overline{\eta}\left(\frac{1}{\eta_g^2}-\frac{1}{\eta_l^2}\right)B_n^2\right)\delta(\phi)\vec{n} \quad (22)$$

where $\overline{\eta}$ is defined as [9]:

$$\overline{\eta}=\begin{cases}\eta_g & \phi>0\\ \eta_l & \phi<0\end{cases} \quad (23)$$

4. Surface Tension Modeling

The surface tension force denoted by $\vec{F}$ as a body force in Eq. (2) is calculated according to the continuum surface force (CSF) method [18] and is expressed as [16,18]:

$$\vec{F}=\kappa\sigma\vec{n}\delta(\phi) \quad (24)$$

where σ is the surface tension coefficient and κ is the interface curvature which is defined as [15,16]:

$$\kappa=\vec{\nabla}\cdot\vec{n} \quad (25)$$

5. Boundary Conditions

Hydrodynamic boundary conditions for the boundaries of the

computational domain are obtained by superposition of the no-slip and no-penetration boundary conditions defined, respectively, as below [19]:

$$\vec{V}\cdot\vec{n}=0 \tag{26}$$

$$\vec{V}\times\vec{n}=0 \tag{27}$$

Boundary condition of the magnetic field equation in all boundaries, except the boundary where the magnetic field is applied, is defined as [9]:

$$\vec{B}\cdot\vec{n}=0 \tag{28}$$

6. Solving Method of the Governing Equations

For solving the governing equations described in section 3, a full computer code was developed in this research. In this code, the governing equations of the flow field of the problem, namely continuity and momentum equations, were discretized by making use of the finite volume method using the SIMPLE algorithm. Also, finite difference method was employed for discretizing the governing equation of the magnetic field.

Like other published numerical studies in this field [9,20], the CPU run time by developed code in this research is also quite long. Simulations were performed on a 3.4-GHz Core i7- 4930k personal computer with 8-GB RAM. Run-time of the cases simulated in this research was about 4-5 weeks. The high run-time was caused by two major factors. The first reason is the magnetic source term added to momentum equation, which results in high run-time in magnetohydrodynamic problems. Another reason is solving the interfaces simulation equations, which leads to high run-time in the numerical study of multiphase flows. In this investigation, which is a two-phase magnetohydrodynamic problem, the combination of these two factors causes high run-time.

RESULTS AND DISCUSSION

By solving the governing equations expressed in section 3, the coalescence and interactions of a pair of gas bubbles rising side by side in a viscous quiescent liquid are investigated. First results of this research were compared with available numerical and experimental results of previously published studies to verify the results of the current numerical simulation. Then, the effects of uniform magnetic fields with different magnitudes were investigated on the interaction of the side-by-side rising bubbles.

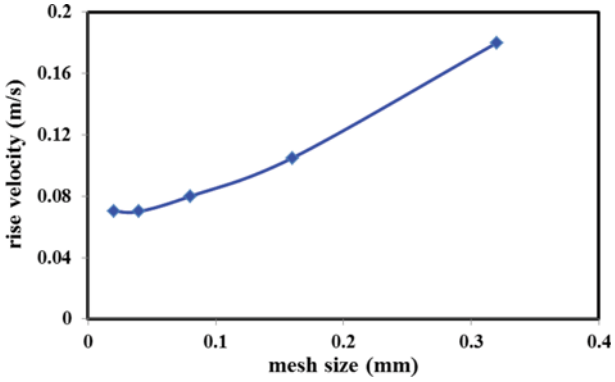

Fig. 2. Mesh independency for numerical simulation of side-by-side rising bubbles.

1. Results Validation

Before numerical simulation of the problem, first the test of mesh independency was conducted and results are shown in Fig. 2. A uniform structured mesh was used for the discretization of the computational domain. Different mesh sizes were used, and it was concluded that when the mesh size is equal to 0.04 mm, the rise velocity of the coalesced bubble (the bubble obtained by the coalescence of two initial bubbles) is independent of the mesh size. Therefore, this mesh size was adapted as a correct mesh size for numerical solving of the governing equations. Note that by using the appropriate mesh size, time step, reinitialization equation and high accuracy discretization methods described in section 3, mass dissipation of the level set method is controlled. The maximum values of mass dissipation of the cases of no-magnetic field effect and under uniform magnetic field effect were less than 3% and 5%, respectively, which is acceptable. Based on the reported researches [14,21], if the mass loss of the level set is less than 10%, it is acceptable and without using re-initialization methods, it may be more than 80% in complex topologies [14,21].

To validate the precision of the developed computer, the reported experimental results of Duineveld [3] and numerical results of Chen et al. [10] were selected for comparison. The reported experimental results of Duineveld [5] specify the behavior and interaction of two air bubbles rising side by side in the hyper-filtrated water. The lack of impurities in this case allows for a meaningful comparison between the experiments and numerical simulations. Therefore, the experimental results of the Duineveld [3] were considered for the sake of comparison of the simulation results obtained in this research. The Morton and Eotvos number of the considered case study are 1.85×10^{-5} and 0.4, respectively, according to the conditions considered in Duineveld [3].

Generally, the dynamics of the bubbles are represented by using two dimensionless numbers, Eotvos (Eo) and Morton (M) numbers, defined respectively as [14]:

$$\mathrm{Eo}=\frac{g\Delta\rho d_e^2}{\sigma} \tag{29}$$

$$\mathrm{M}=\frac{g\mu_l^4\Delta\rho}{\rho_l^2\sigma^3} \tag{30}$$

In Eqs. (29) and (30), $\Delta\rho$ denotes the density difference of liquid and gas phases.

The results of this research were compared with the reported numerical results of Chen et al. [10] and experimental results of Duineveld [3]. As shown in Fig. 3, there is a good qualitative agreement between the computed results of the present study and the results of Chen et al. [10] and Duineveld [3]. When two side-by-side rising bubbles approach to each other, a thin liquid film is formed between them before coalescence occurs. The emerging pressure inside the separating thin film of bubbles will increase by getting close to each other, and consequently a resisting and repulsive force will appear between two bubbles. This thin film, which is referred as "dimple" and also repellent force between a pair of bubbles, plays an important role in the interaction between them. As mentioned

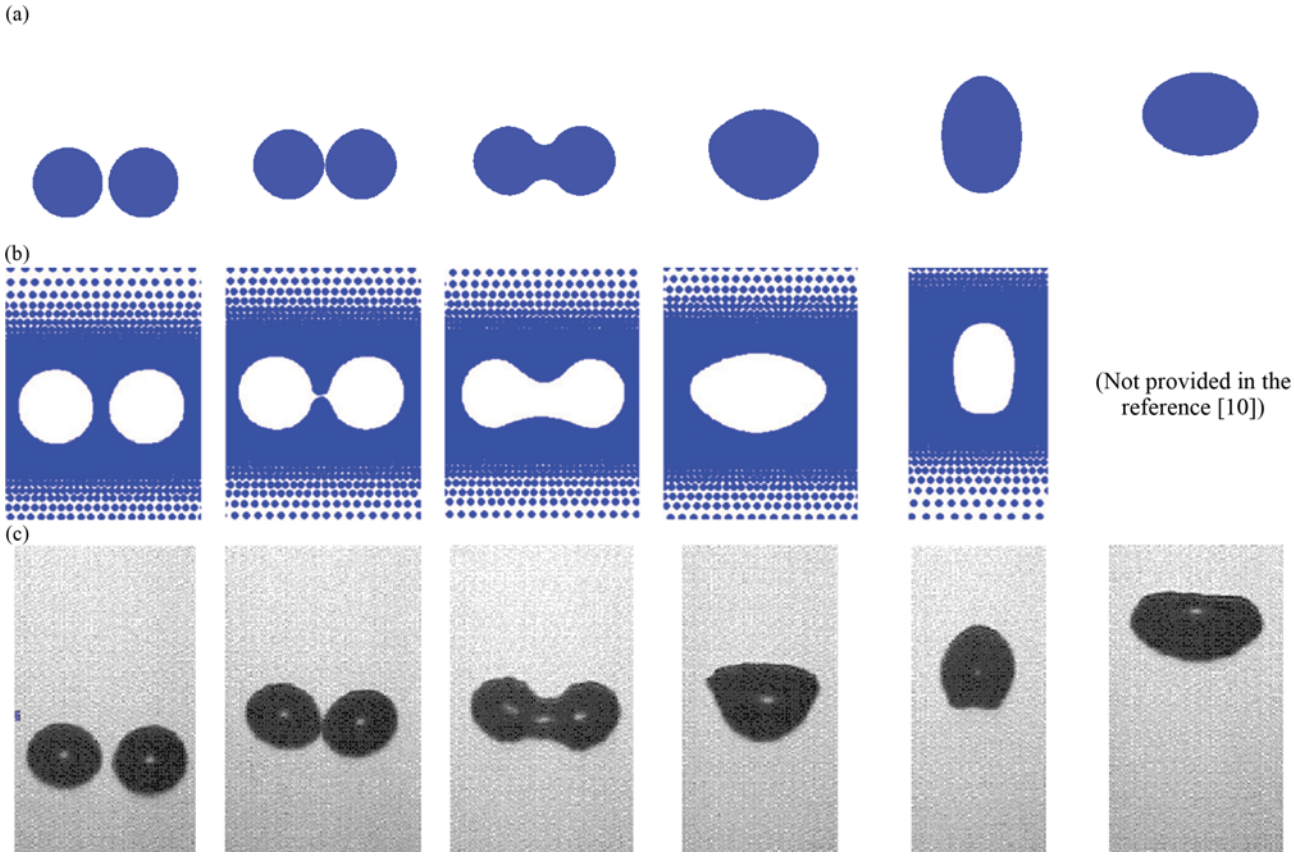

Fig. 3. Comparison of the coalescence of side-by-side rising bubbles obtained in this research with numerical and experimental results; (a) results of present research using the Level Set method; (b) numerical results of Chen et al. [10] obtained using the MPS method, (c) experimental results taken from [3].

in the previous studies [3,22], two parallel rising bubbles will coalesce with each other when the inertia of bubbles can overcome that repellent force.

2. Side-by-side Interaction of a Pair of Bubbles under Effects of the Uniform Magnetic Field

Movement, interaction and finally, the coalescence of a pair of gas bubbles rising freely side by side in a stagnant viscous liquid due to buoyancy force were investigated and the results shown and discussed in the previous section. In this section, effects of magnetic field on the same problem are studied, and the results are compared with the free rising bubbles' case.

The effects of different strengths of uniform magnetic field up to 0.1 T on the dynamics, deformation and interaction of the pair of bubbles described in sections 2 and 4.1 are shown and compared with the case of no-magnetic field effects in Fig. 4. The first row of Fig. 4 represents the free side-by-side rising bubbles under the effect of buoyancy in the liquid column at different time instants. The bubbles and surrounding liquid initially are at rest. As the bubbles are released, they rise due to the buoyancy force. During rising in the stagnant liquid, a flow field is induced in the adjacent surrounding liquid due to the movement of the bubbles. The induced flow field is focused on the region near the upper surface of the bubbles due to their upward motion where the downward regions of the bubbles are still stagnant nearly. Therefore, the velocity of the liquid in the upper region of the bubbles is higher in comparison to other regions, especially the underside of the bubbles. So, the liquid flows through the gap between the bubbles. During this flow, the pressure decreases in the gap and causes attractive forces acting on the bubbles. These attractive forces pull the bubbles to each other, and as a result, the minimum distance between them decreases during their free rising in a flow domain without any magnetic field. This phenomenon is shown clearly in the first row of Fig. 4 for case b=0.0T. The reduction of the distance between the bubbles continues until the bubbles reach each other and coalescence occurs between them at about t=0.053 sec. The pressure distributions on some horizontal lines at the entrance of the gap between the bubbles for case of Fig. 4 are presented in Fig. 5 at t=0.009 sec. Pressure distribution at the level of y=2 mm is illustrated in Fig. 5(b). This level (y=2 mm) is close to the neck of converge-diverge gap between the bubbles, which is specified in Fig. 5(a). The pressure difference between the liquid in the gap and surrounding liquid of the bubbles is specified by *DP* in the figure. As shown in Fig. 6(b), the amount of pressure in the gap between the bubbles is less than that in the surrounding at y=2 mm; therefore, the induced force by this pressure difference will push the bubbles to each other. So, the bubbles approach each other during the rising in the liquid column. As explained, by decreasing the width of the initial gap between the bubbles during the rising of them, the mentioned attrac-

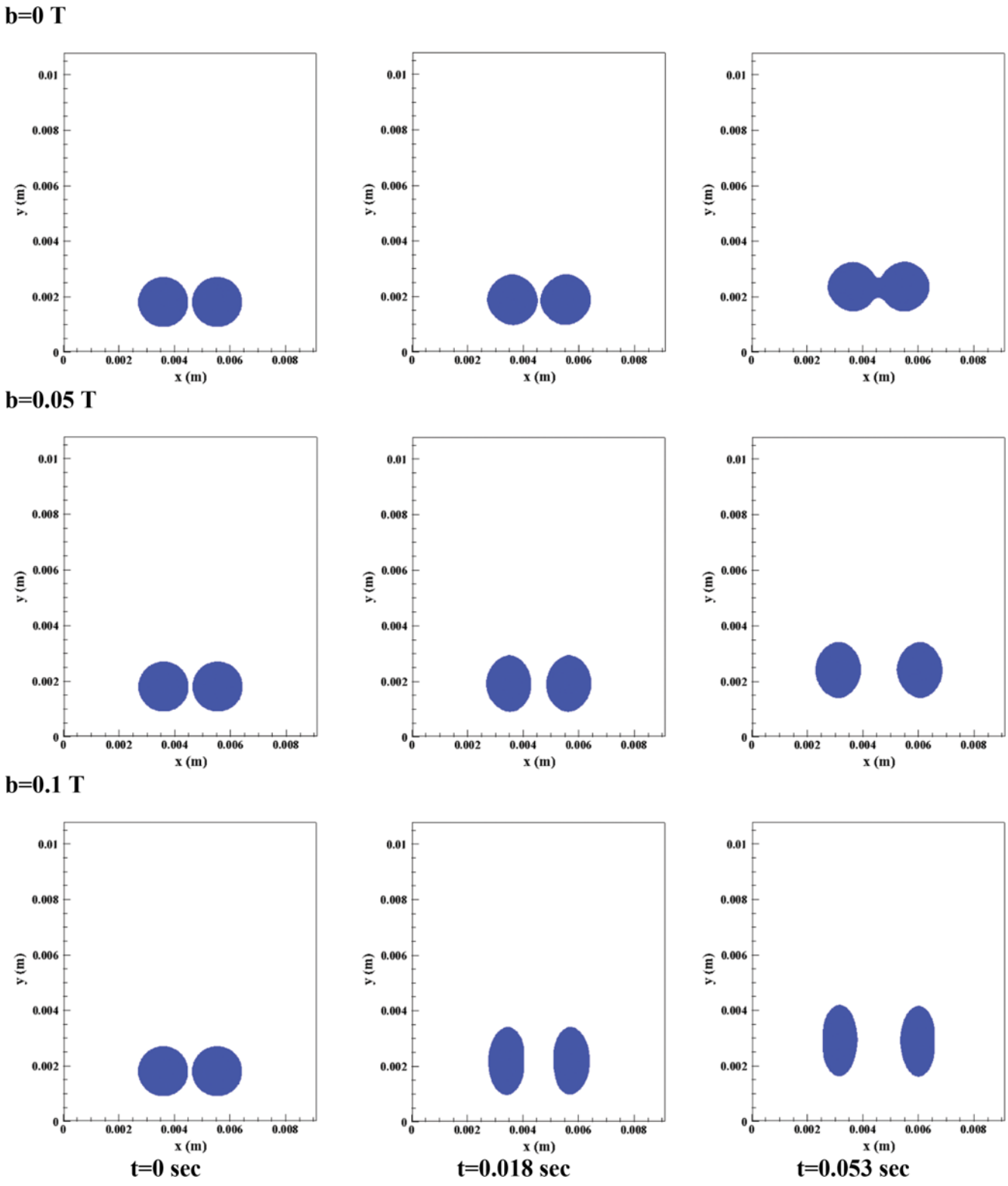

Fig. 4. Effects of different magnitudes of the magnetic field on the interaction of the side-by side-pair of bubbles at various time instants.

tive forces will dominate the repelling forces which are caused due to the flow blocking in the gap between the bubbles. Hence, the bubbles got closer and closer during the rising in the liquid column. Two peaks in pressure distributions depicted in Fig. 5 are pressure differences between the inside of bubbles and surrounding liquid caused due to the surface tension forces acting on the bubbles. The pressure distribution at the levels y=2.4 mm and y=2.6 mm are shown in Fig. 6(c) and 6(d), respectively, which are roughly

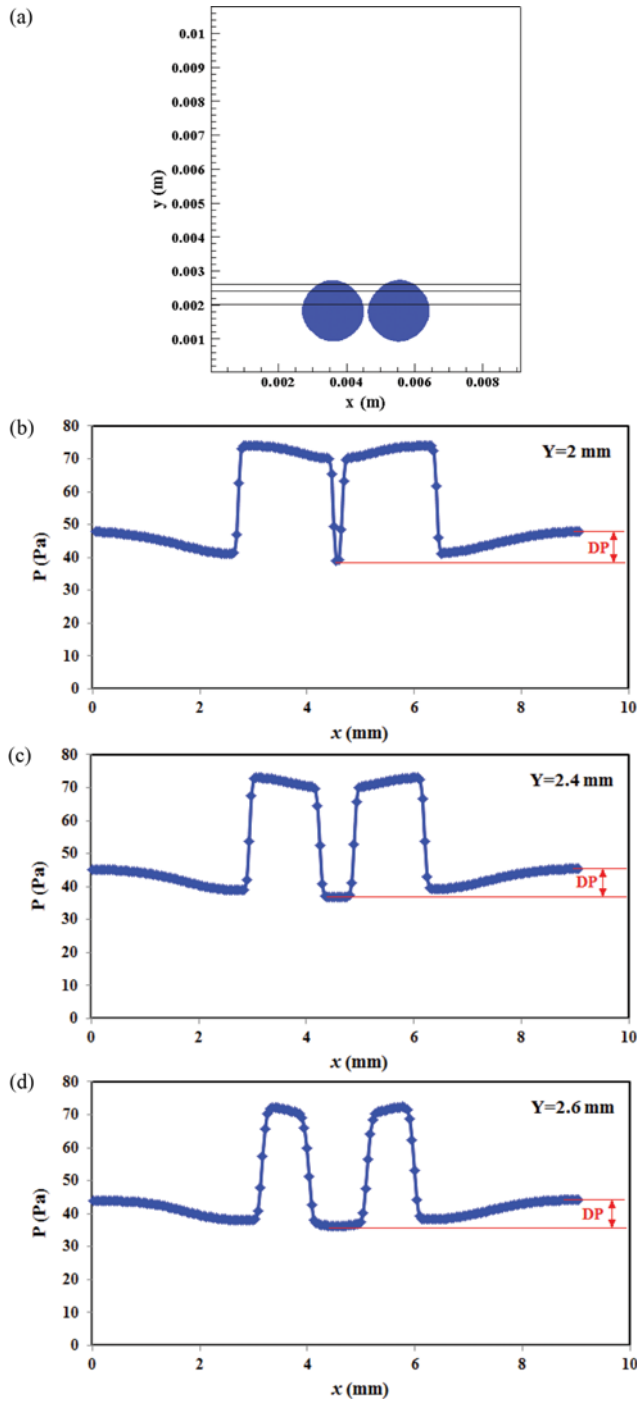

Fig. 5. Pressure distribution in the flow field of side-by-side rising bubbles at different vertical positions in the absence of magnetic field at t=0.009 sec; (a) horizontal lines of the geometry where the pressure distributions are depicted; (b, (c), (d) pressure distribution on the horizontal lines of y=2 mm, y=2.4 mm and y=2.6 mm respectively.

the same as each other. The effects of magnetic fields with strengths of 0.05 T and 0.1 T on the interaction of two rising bubbles are shown in the rows 2 and 3 in Fig. 4, respectively. As illustrated in Fig. 4, because of magnetic permeability differences between two phases, the applied uniform magnetic field will elongate the bubbles in the

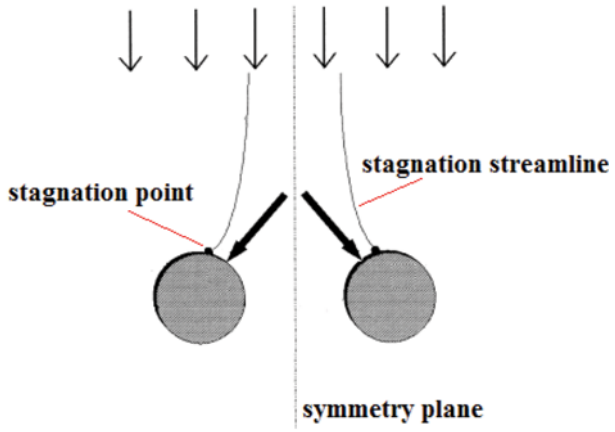

Fig. 6. Stagnation points and repelling force on side-by-side rising bubbles [23].

vertical direction. Note that the resistance of gas phase inside the bubbles against the magnetic field is higher than that of the liquid phase, so the magnetic field lines tend to pass through the liquid phase. By rising up of the bubbles, the magnetic field will reduce their cross section [8,9]. The distance between the elongated bubbles will increase because of reducing their cross section. There is a direct link between the magnetic field strength and the vertical elongation of bubbles. As shown in Fig. 5, by increasing the magnitude of magnetic strength the bubbles have been more slender and the width of the gap between them increased. As the horizontal distance between the bubbles increases, the effect of the low pressure region on the bubbles at the entrance of the gap between them is reduced; therefore, the interactions and attraction forces between bubbles will weaken and consequently, the bubbles because of repelling force of the stagnation points and flow blocking between them will diverge from each other as they rise in the column. In the case of single bubble rising, the stagnation point is located in the symmetry plane of the bubble, but in the side-by-side rising of two bubbles as illustrated in Fig. 6, the stagnation points of the bubbles are oriented slightly to the symmetry plane of the entire geometry [3,23]. Note too that the bubbles rising in a stagnant liquid are similar to the stagnant bubbles exposed to the liquid flow (in the viewpoint of stagnation points) as shown in Fig. 6. In this case, the horizontal components of pressure forces on the bubbles surface will act as repulsive forces, and therefore in a parallel rising, the bubbles will diverge from each other. The behavior of the magnetic field lines of cases which are presented in Fig. 4, are shown in Fig. 7 at the same time instants for the same conditions (b=0.03 T, 0.05 T and 0.1 T). As shown in Fig. 7, magnetic field lines deform when they reach to the bubbles and tend to pass through the path which has low resistance against the magnetic field. Therefore, the density of magnetic field lines in the gas phase is lower than that of the liquid phase. The difference in the density of magnetic field lines in two different phases induces a force which only acts at the interface of the two phases [8,9].

Vectors and contours of the magnetic field forces are shown in Figs. 8 and 9, respectively. As illustrated in Fig. 8, the vectors of magnetic field force are toward the inside of the bubbles because of the direction of the magnetic field gradient (gradient of the magnetic

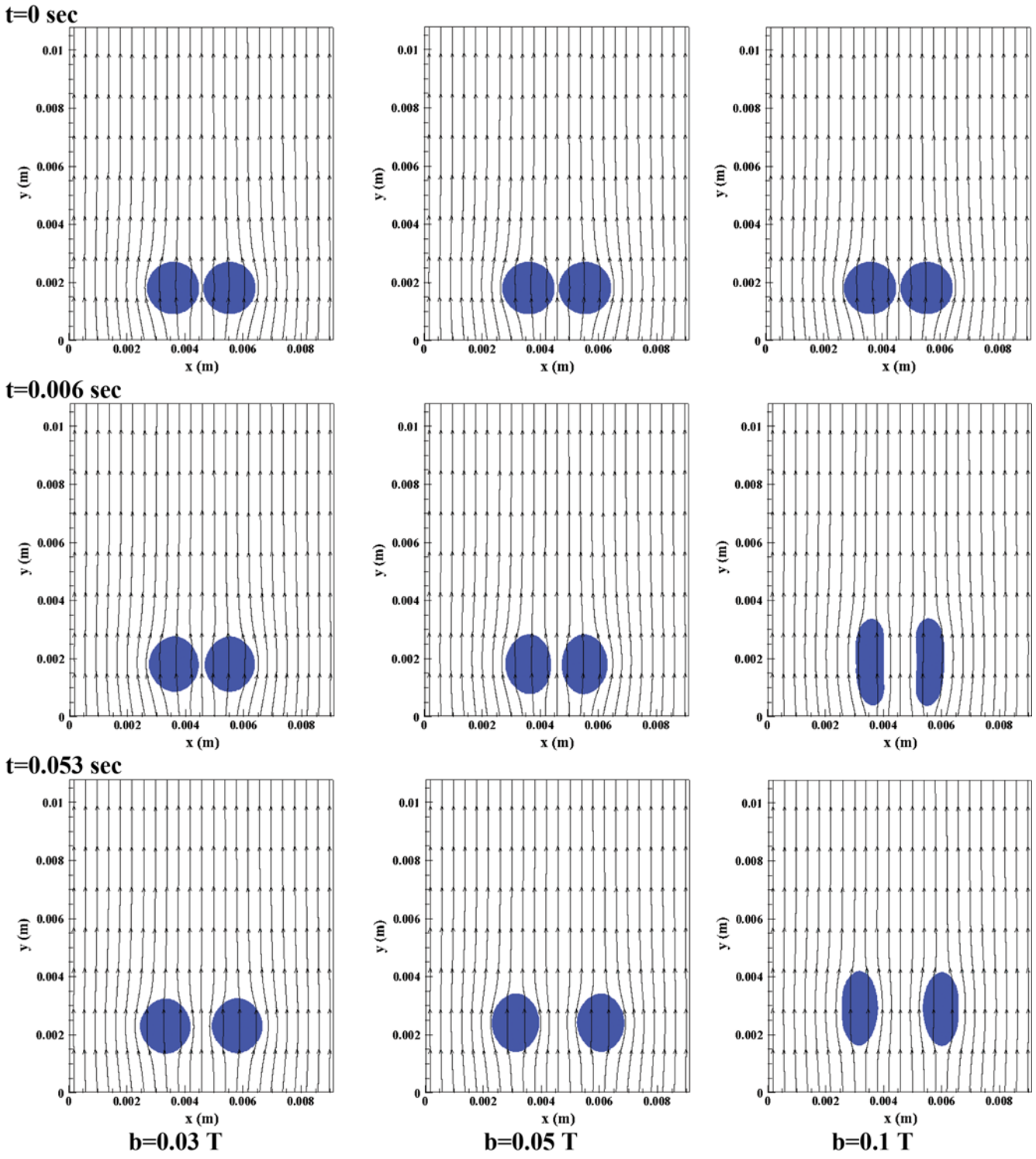

Fig. 7. Magnetic field lines at different time steps and magnitudes of magnetic fields.

field is negative in the direction toward the inside of bubbles). From Fig. 8, the concentration and also deformation of magnetic field lines on the sides of bubbles are greater than the amount of those on the upper and lower surfaces of bubbles. Therefore, the magnetic field gradient and also the exerted magnetic force to the sides of bubbles are greater than those which act on upper and lower surfaces of bubbles. By the above explanation, the net effect of magnetic force on the interface of two side by side rising bubbles is horizontal compression and vertical elongation of the bubbles. As the strength of the magnetic field increases, the magnetic force induced to the interface of the bubbles increases and deformation of the bubbles and also their vertical elongation increases. Magnetic force contours are presented in Fig. 9. The magnetic field forces act only at the interface of the two phases so the amount of this force inside

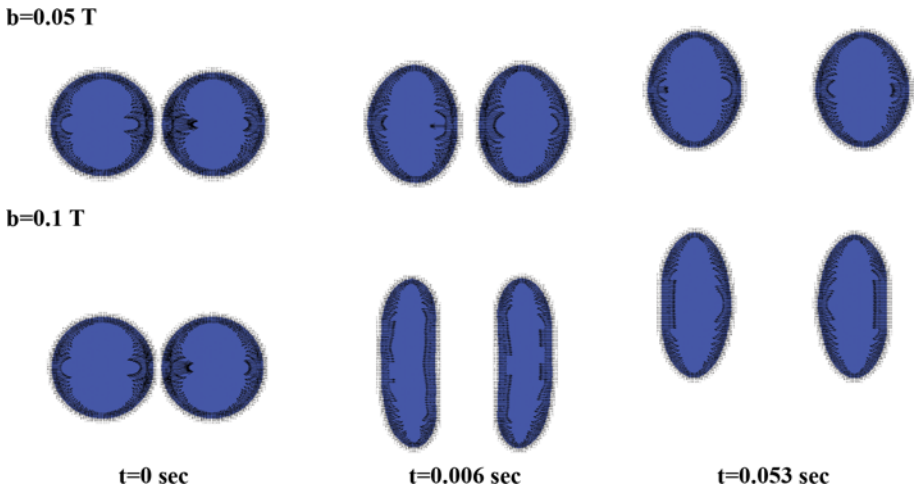

Fig. 8. Magnetic field force vectors at different time steps and magnitudes of magnetic fields.

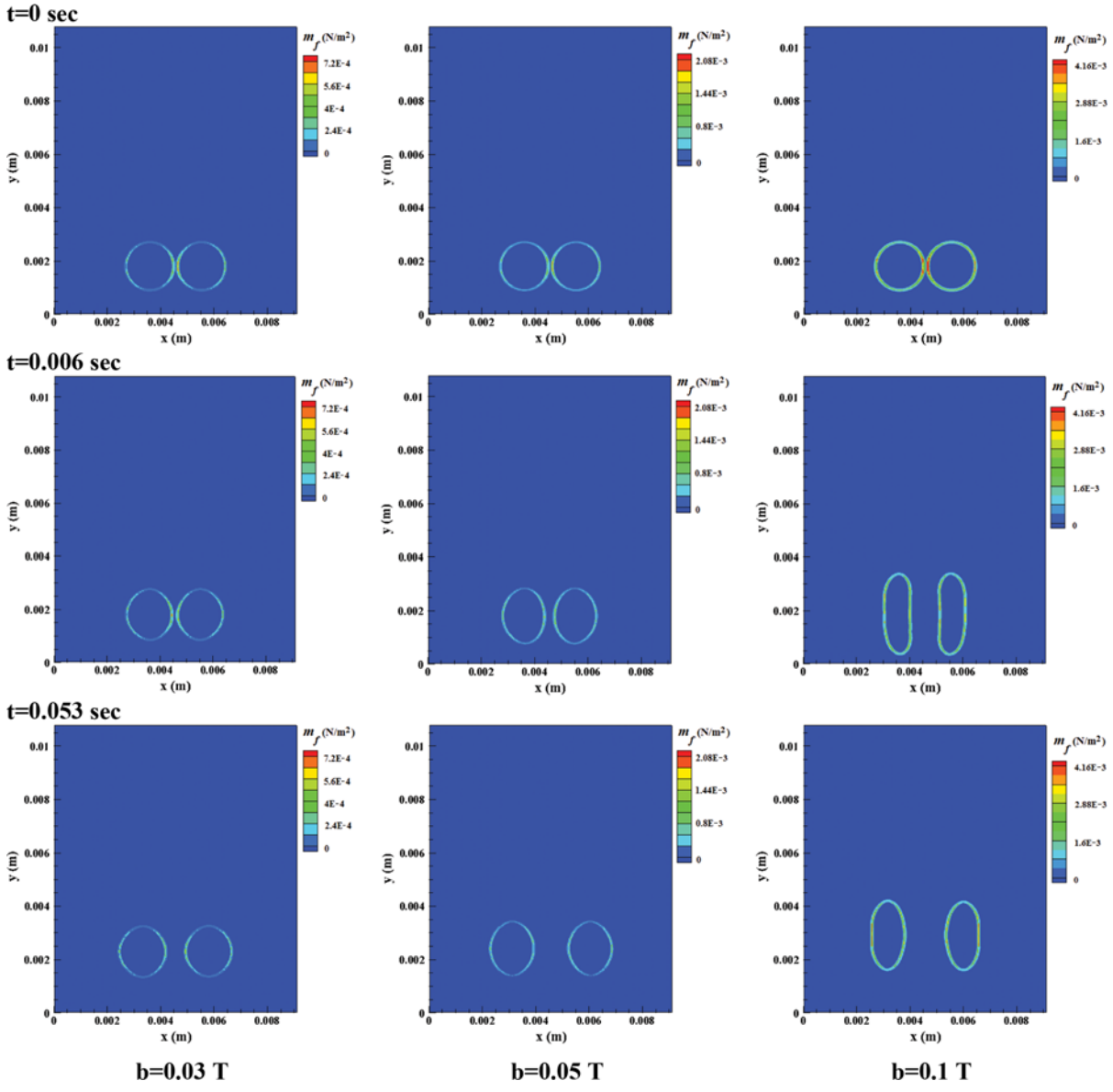

Fig. 9. Magnetic field force contours at different time steps and magnitudes of magnetic fields.

the bubble (gas phase) and the surrounding (liquid phase) is zero. With reference to Fig. 9, it is obvious that the magnitude of the magnetic field force is higher on the two sides of the bubble in comparison to the other parts of that, and also Fig. 9 clearly shows that the magnetic field force on the adjacent sides of the bubbles is higher than that on opposite sides close to the walls (t=0 sec to t= 0.006 sec in the case of b=0.03 T). From Fig. 9, when the distance between the bubbles increases, the distribution of the magnetic field force at the interface of bubbles near the gap becomes almost symmetric. By comparison of the magnetic force contours of cases b=0.03 T, b=0.05 T and b=0.1 T, it is revealed that the magnitude of the magnetic field force increases by increasing the strength of the magnetic field.

CONCLUSION

Results show that the applied external uniform magnetic field elongates the bubbles in the direction of the magnetic field, and consequently results in increasing of the minimum distance between them. As the coalescence of rising bubbles strongly depends on the minimum distance between them, therefore, the possibility of coalescence occurring between a pair of bubbles rising side by side in a magnetic field is less than that in a domain without any magnetic field. Elongation and enhancement of the bubbles' rise velocity depend on the strength of the applied magnetic field. Enhancement of about 50% in mean rise velocity of the bubbles is observed in the case of applied magnetic fields with the strength of 0.1 T. As the different regimes of two-phase flows have different hydrodynamic and heat transfer behavior, the applied external uniform magnetic field, which is able to control the coalescence of bubbles, can play an important role in controlling of the two-phase flows characteristics. In summary, the main findings of the present research are:

- Dielectric gas bubbles are elongated in the direction of applied uniform magnetic fields.
- Applications of uniform magnetic fields prevent bubbles forming side-by-side coalescence.
- The rise velocity of bubbles enhances in a dielectric two-phase flow in presence of uniform magnetic fields which is a function of strength of applied magnetic field.

ACKNOWLEDGEMENT

The authors would like to acknowledge the financial support by Sahand University of Technology during this research.

NOMENCLATURE

B, b : magnetic field in flow field-magnetic flux density [T]
D : rate of strain tensor [1/s]
Eo : Eotvos number
F : surface tension force [N/m^3]
g : gravity acceleration [m/s^2]
H : external magnetic field [A/m]
J_c : electric current [A]
M : morton number
m_f : magnetic field force [N/m^2]
n : unit normal vector
p : pressure [Pa]
Re : Reynolds number
T : magnetic field source term [N/m^3]
t : time [sec]
V : velocity vector [m/s]
x, y : coordinate components [m]

Greek Symbols

α : numerical constant
Δx : grid step [m]
Γ : interface
ε : thickness of the interface [m]
η : magnetic permeability [T·m/A]
κ : curvature of the interface [1/m]
μ : dynamic viscosity [Pa·s]
ξ : component of potential vector
ρ : density [kg/m^3]
σ : surface tension coefficient [N/m]
ϕ : level Set function [m]

Subscripts

g : gas phase
l : liquid phase

REFERENCES

1. H. Z. Li, Y. Mouline, L. Choplin and N. Midoux, *Int. J. Multiphase Flow*, **23**, 713 (1997).
2. J. Liu, C. Zhu, T. Fu, Y. Ma and H. Li, *Chem. Eng. Sci.*, **93**, 55 (2013).
3. P. C. Duineveld, *App. Sci. Res.*, **58**, 409 (1998).
4. R. K. Das and S. Pattanayak, *Chem. Eng. Sci.*, **49**, 2163 (1994).
5. A. Ramos-Banderas, R. D. Morales, R. Sanchez-Perez, L. Garcıa-Demedices and G. Solorio-Diaz, *Int. J. Multiphase Flow*, **31**, 643 (2005).
6. W. Xie, R. Li, X. Lu, P. Han and S. Gu, *Korean J. Chem. Eng.*, **32**, 643 (2015).
7. K. Alinezhad, M. Hosseini, K. Movagarnejad and M. Salehi, *Korean J. Chem. Eng.*, **27**, 198 (2010).
8. H. Ki, *Comput. Phys. Commun.*, **181**, 999 (2010).
9. M. R. Ansari, A. Hadidi and M. E. Nimvari, *J. Magn. Magn. Mater.*, **324**, 4094 (2012).
10. R. H. Chen, W. X. Tian, G. H. Su, S. Z. Qiu, Y. Ishiwatari and Y. Oka, *Chem. Eng. Sci.*, **66**, 5055 (2011).
11. M. Sussman, E. Fatemi, P. Smereka and S. Osher, *Comput. Fluids*, **27**, 663 (1988).
12. J. H. Kim, K. H. Ahn and S. J. Lee, *Korean J. Chem. Eng.*, **8**, 1010 (2012).
13. E. Marchandise, P. Geuzaine, N. Chevaugeon and J. Remacle, *J. Comput. Phys.*, **225**, 949 (2007).
14. M. R. Ansari and M. E. Nimvari, *Ann. Nucl. Energy*, **38**, 2770 (2011).
15. S. Osher and J. A. Sethian, *J. Comput. Phys.*, **79**, 12 (1988).
16. M. Sussman, P. Smereka and S. J. Oshe, *J. Comput. Phys.*, **114**, 146 (1994).
17. F. Melia, *Electrodynamics*, The University of Chicago Press, Chi-

cago (2001).
18. J. U. Brackbill, C. Kothe and D. B. Zemach, *J. Comput. Phys.*, **100**, 335 (1992).
19. G. H. Golub, A. Greenbaum, A. M. Stuart and E. Suli, *Mathematical methods for the magneto hydrodynamics of liquid metals*, Oxford University Press (2006).
20. H. L. Huang, A. Ying and M. A. Abdou, *Fusion Eng. Des.*, **63**, 361 (2002).
21. K. B. Deshpande and W. B. Zimmerman, *Chem. Eng. Sci.*, **61**, 6486 (2006).
22. A. K. Chesters and G. Hofman, *Appl. Sci. Res.*, **38**, 353 (1982).
23. R. Folkersma, H. N. Stein and F. N. Vosse, *Int. J. Multiphase Flow*, **26**, 877 (2000).